Earth and Planetary Science Letters 283 (2009) 122–132

Contents lists available at ScienceDirect

Earth and Planetary Science Letters

journal homepage: www.elsevier.com/locate/epsl

Non-chondritic HSE budget in Earth's upper mantle evidenced by abyssal peridotites from Gakkel ridge (Arctic Ocean)

Chuan-Zhou Liu [a,b,*], Jonathan E. Snow [b,c], Gerhard Brügmann [b], Eric Hellebrand [b,d], Albrecht W. Hofmann [b]

[a] State Key Laboratory of Lithospheric Evolution, Institute of Geology and Geophysics, Chinese Academy of Sciences, Beijing, 100029, China
[b] Max-Planck Institut für Chemie, Abteilung Geochemie, Mainz, 55020, Germany
[c] Department of Geosciences, University of Houston, Houston, Texas 77204, USA
[d] Department of Geology and Geophysics, University of Hawaii, Honolulu, Hawaii 96822, USA

ARTICLE INFO

Article history:
Received 14 January 2009
Received in revised form 2 April 2009
Accepted 3 April 2009
Available online 6 May 2009

Editor: R.W. Carlson

Keywords:
HSE
abyssal peridotites
Gakkel ridge
PUM

ABSTRACT

Constraints on the highly siderophile element (HSE: including Os, Ir, Ru, Pt, Pd and Re) budget of the upper mantle upwelling beneath mid-ocean ridges have until now been based on samples that have experienced varying degrees of alteration, partial melting and secondary igneous processes. Here we present results from a set of abyssal peridotites that have been relatively unaffected by these phenomena. Eighteen abyssal peridotites from two localities along the ultra-slow spreading Gakkel Ridge (Arctic Ocean) were selected for this study. Samples from one locality (PS66-238) are extremely fresh, while those from HLY0102-D70 are typical abyssal serpentinites. Comparison of HSE data between fresh peridotites and weathering products supports the contention that HSE are stable during serpentinization, but that Pd and Re are mobile during subsequent weathering. HSE budgets of spinel lherzolites suggest that all platinum group elements (PGEs: including Os, Ir, Ru, Pt and Pd) are compatible during very low degree of partial melting (5–8%), whereas Re behaves as an incompatible element. Harzburgites from each locality were subjected to ~12% fractional partial melting, which is lower than that expected for total consumption of sulfides in mantle peridotites (ca. 16%). The harzburgites are depleted in PPGE (Pt, Pd) and Re relative to IPGE (Os, Ir, Ru), which reflects the extraction of sulfide melt along with the silicate melt.

Low bulk-rock contents of both Na_2O and TiO_2 in the fresh PS66-238 lherzolites indicate that they were not transformed from harzburgites through melt refertilization, but represent pristine fertile mantle rocks. Their systematic suprachondritic Ru/Ir and Pd/Ir ratios, but chondritic Pt/Ir ratios, cannot be ascribed to partial melting or secondary igneous processes. This signature may reflect the primary HSE signature of the Earth's upper mantle. Non-chondritic HSE patterns discovered in PS66-238 lherzolites are consistent with the primitive upper mantle (PUM) inferred from the study of orogenic peridotites and mantle xenoliths.

1. Introduction

It is well known that the iron-loving highly siderophile elements (HSE) in mantle rocks are capable of providing important information about the characteristics of materials and processes of early Earth accretion and core formation. Due to their high metal/silicate partition coefficients ($D^{M/S}$), HSE in the silicate Earth were almost completely stripped from the mantle during core–mantle separation in the early Earth. For this reason, vanishingly small levels of the HSE (by a factor of about 10^{-6}) are expected to have remained in the modern mantle. However, HSE in mantle peridotites from many different tectonic settings are only approximately 150 times less abundant relative to chondritic meteorites (Jagoutz et al., 1979; Morgan, 1986; Morgan et al., 2001), a much higher concentration than would be expected from metal-silicate equilibrium partitioning. The excess HSE contents, together with their broadly chondritic abundance ratios, have been generally explained by the 'late-veneer' hypothesis (Chou, 1978; Jagoutz et al., 1979; Morgan, 1986; O'Neill, 1991; Schmidt et al., 2000; Holzheid et al., 2000; Meisel et al., 2001; Morgan et al., 2001), in which nearly all HSE in the early Earth have been stripped into the core and the HSE budget in the modern mantle is dominated by late-accreted materials. Other hypotheses, e.g., inefficient core formation (Jones and Drake, 1986) and high-pressure core formation (Murthy, 1991; Righter and Drake, 1997), have also been proposed. Due to the divergent chemical behaviors of the HSE during planetary partitioning processes between metal and silicates, and between solid metals and liquid metals, it is difficult for these models to account for both high abundances of HSE and chondritic HSE ratios in Earth's mantle (Becker et al., 2006). For example, the high-pressure core formation model requires the bulk-earth HSE to have concentrations proportional to metal-silicate partition

* Corresponding author. State Key Laboratory of Lithospheric Evolution, Institute of Geology and Geophysics, Chinese Academy of Sciences, Beijing, 100029, China. Tel.: +86 10 82998547; fax: +86 10 62010846.
E-mail address: chzliu@mail.iggcas.ac.cn (C.-Z. Liu).

0012-821X/$ – see front matter © 2009 Elsevier B.V. All rights reserved.
doi:10.1016/j.epsl.2009.04.002

coefficients for the appropriate pressure range of core formation to account for chondritic HSE ratios in the derived mantle. This is unlikely, owing to the different low-temperature geochemical behaviors of the different HSE on one hand (Lorand et al., 2008), and the current controversy on HSE partitioning at high pressures on the other hand (Cottrell and Walker, 2006; Ertel et al., 2006).

Non-chondritic HSE patterns were first reported in orogenic lherzolites (Pattou et al., 1996) and then in mantle peridotites from different settings (Snow and Schmidt, 1998; Rehkämper et al., 1999; Becker et al., 2006). The models proposed to account for the non-chondritic HSE features remain highly controversial (Snow and Schmidt, 1998; Rehkämper et al., 1999; Luguet et al., 2003). For example, addition of outer-core materials back into the mantle has been proposed to account for the non-chondritic HSE signatures in mantle peridotites (Snow and Schmidt, 1998). Alternatively, Rehkämper et al. (1999) suggested that supra-chondritic Pd/Ir and Re/Ir ratios observed in some mantle peridotites are the result of universal secondary magmatic processes and that the 'late-veneer' hypothesis is thus still viable. Secondary magmatic processes, such as melt percolation, have also been commonly invoked as the cause of the non-chondritic HSE compositions observed in mantle xenoliths and massif peridotites (Lorand et al., 1999; Lorand and Alard, 2001; Lorand et al., 2003; Lorand et al., 2004; Pearson et al., 2004; Ionov et al., 2006).

To circumvent the potential effects of secondary processes, the composition of the primitive upper mantle (PUM), which represents a hypothetical composition for the silicate Earth before any mantle–crust differentiation or mantle-melting event, has been used to discuss the processes occurring in the early Earth. Based on global mantle xenoliths,

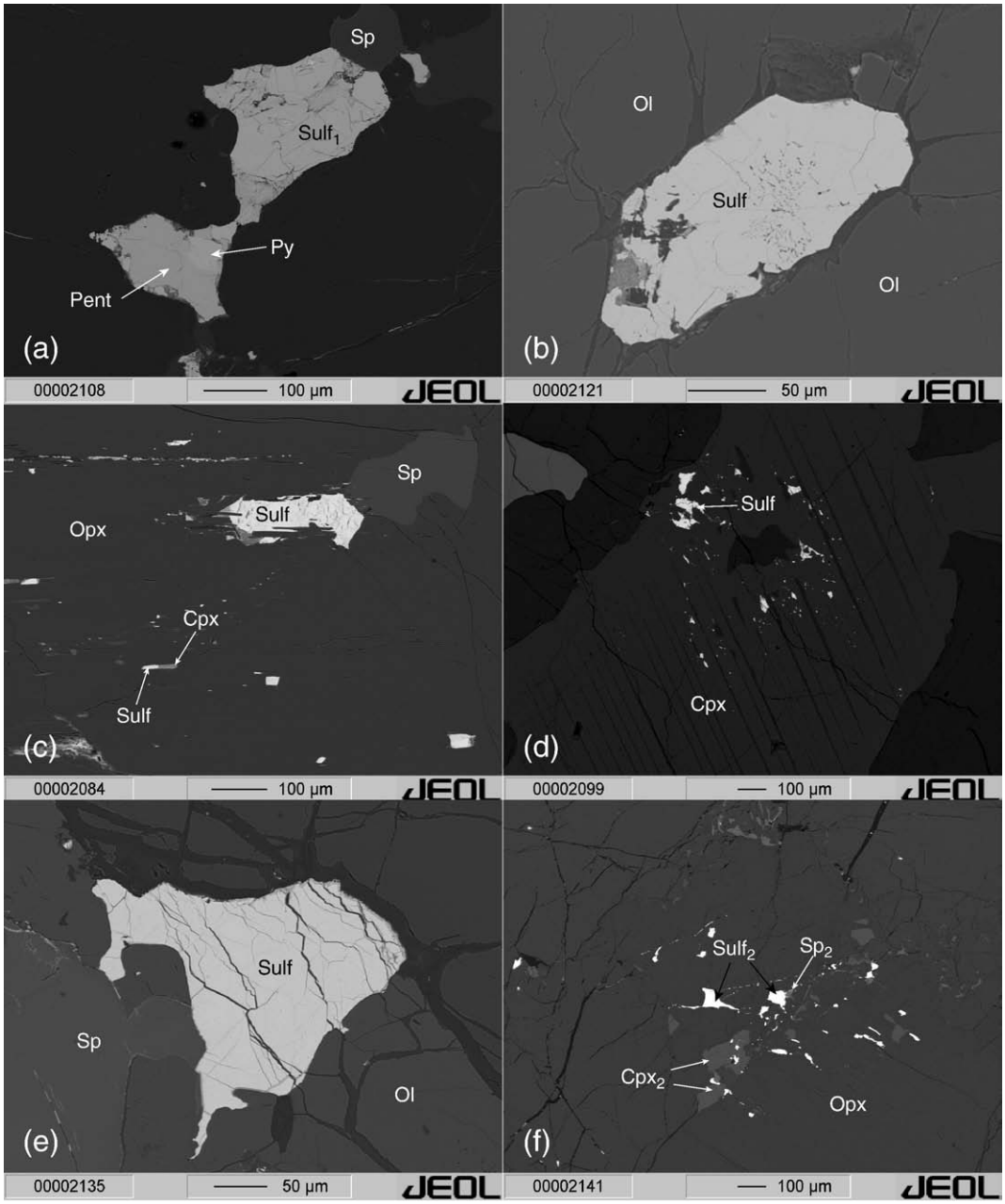

Fig. 1. Backscattered Electron (BSE) image of base metal sulfides (BMS) in fresh Gakkel abyssal peridotites (a–f). (a) blocky pentlandite intergrown with pyrrhotite. (b) sulfide (Pn) included in olivine. (c) small-sized sulfides droplet as little trails of the sulfide inclusions, locating within the fracture planes radiating from these inclusions. (d) tiny sulfides droplets in alignment with the lamellae of clinopyroxene. (e) interstitial sulfides, euhedral to anhedral, disseminating among the silicate and spinel matrix. (f) tiny Cu–Ni-rich sulfides ($Sulf_2$), together with assemblage of little spinel (Sp_2) and cpx (Cpx_2), distributing along the boundary of the opx and/or olivine. Py = pyrrhotite; Pent = pentlandite; Ol = olivine; Opx = orthopyroxene; Cpx = clinopyroxene; Sp = spinel; Sulf = sulfide.

the $^{187}Os/^{188}Os$ ratios of the modern PUM have been inferred to be similar to those of some ordinary and enstatite chondrites but are distinctly higher than the ratios in carbonaceous chondrites. This suggests that the late accreted materials had nebular histories most like those of ordinary and enstatite chondrites, rather than carbonaceous chondrites (Meisel et al., 1996; Meisel et al., 2001). By the use of massif peridotites and mantle xenoliths, Becker et al. (2006) inferred that the PUM has a non-chondritic HSE pattern, which is different from those of the known chondrites. The reliability of including the composition of massif-type lherzolites to estimate the PUM, however, has been recently questioned (Lorand et al., 2008), because many orogenic lherzolites are secondary rocks resulting from melt refertilization rather than pristine mantle rocks (Le Roux et al., 2007).

Mantle rocks that have experienced relatively little melt depletion and melt refertilization are ideal to constrain the HSE compositions of the PUM. For this reason, we have conducted a study of abyssal peridotites from Gakkel Ridge, Arctic Ocean, most of which are fertile lherzolites that experienced little melt extraction or late refertilization. Furthermore, samples from one dredge haul are extremely fresh.

2. Sample descriptions

Gakkel Ridge is the slowest-spreading mid-ocean ridge in the world, with full spreading rates ranging from 1.4 cm/yr at the western end to 0.7 cm/yr at the eastern end (Michael et al., 2003). Samples in the present study were selected from two dredge hauls, HLY0102-D70 and PS66-238, from which Os isotopes have previously been reported (Liu et al., 2008). Dredge haul HLY0102-D70 was recovered in 2001 during the US–German Joint AMORE 2001 cruise, and represents the easternmost peridotites collected from Gakkel Ridge. Dredge haul PS66-238 was recovered in 2004 during PFS Polarstern cruise ARK XVII-2 from the 'amagmatic' western end of the Sparsely Magmatic Zone (3°E–8°E). In this region, no basalt but only mantle peridotites have been recovered (Snow and Petrology-Group-ARK-XX-2, 2007), and the seismic crust is inferred to consist entirely of variably serpentinized peridotite (Jokat et al., 2003).

Samples selected from dredge PS66-238 comprise nine spinel lherzolites, one plagioclase lherzolite and one harzburgite. Notably, they are extremely fresh with little to no detectable serpentine in thin section. Each sample, however, has a rim of a cm-thick brown-yellow weathered rock. Most fresh interiors have loss on ignition (LOI) close to 0, with only two of them around 1%. The altered rims have slightly higher LOI (<3%) relative to their corresponding interiors, but still much lower than those of the typical serpentinites (>10%). Samples from dredge HLY0102-D70, consisting of six lherzolites and one harzburgite, are typical serpentinites with LOI of 9–14%.

All PS66-238 samples were examined for base-metal sulfides (BMS) under the microscope. Lherzolites have higher modal contents of sulfides than the harzburgite. Blocky pentlandite is by far predominant and compositionally homogeneous, and sometimes intergrown with pyrrhotite (Fig. 1a). Occurrences of BMS in Gakkel peridotites are similar to those observed from orogenic peridotites and mantle xenoliths, i.e., they are either included in silicates or interstitial among silicate matrix (Griffin et al., 2004; Lorand and Gregoire, 2006). Sulfides included in silicates or spinels are generally rounded to euhedral single sulfide blebs, with diameters up to 200 μm (Fig. 1b). Consistent with previous observations (Lorand and Gregoire, 2006), these sulfide inclusions are commonly surrounded by fracture planes, which may or may not communicate with the grain boundaries of host silicates. These fracture planes are also preferential pathways for later serpentinization of abyssal peridotites, and possibly result from differential contraction of silicates and enclosed sulfides during cooling (Andersen et al., 1987; Dromgoole and Pasteris, 1987). Tiny (1–20 μm in diameter) sulfide droplets are located within the fracture planes radiating from these inclusions (Fig. 1c). In particular, some are distributed in alignment with the lamellae of pyroxenes (Fig. 1d). Small sulfides sometimes are also included within the recrystallized areas of clinopyroxenes. Sulfides interstitial or disseminated within the silicate matrix are euhedral to anhedral in shape, with maximum size up to 200 μm (Fig. 1e). Small sulfides, together with secondary spinels (sp_2) and cpx (cpx_2), can be observed to be interstitial along the boundary of pyroxene and olivine (Fig. 1f), which

Table 1
Whole-rock major elements of D70 and PS66-238 samples.

Sample	Cruise #	Lithology	SiO_2	TiO_2	Al_2O_3	Cr_2O_3	FeOt	MnO	MgO	NiO	CaO	Na_2O	K_2O	LOI	Total	Mg#
D70-56	HLY0102	Sp LH	38.41	0.03	1.79	0.40	7.76	0.11	36.10	0.27	2.14	0.12	0.01	13.53	100.68	0.89
D70-58	HLY0102	Sp LH	41.38	0.08	2.90	0.42	8.16	0.12	34.77	0.27	3.24	0.14	0.01	9.40	100.88	0.88
D70-62	HLY0102	Sp HZ	38.81	0.03	1.13	0.30	7.63	0.12	38.04	0.29	0.35	0.13	0.01	13.77	100.62	0.90
D70-64	HLY0102	Sp LH	38.90	0.03	1.47	0.32	7.94	0.09	37.63	0.29	1.29	0.10	0.01	12.71	100.76	0.90
D70-73	HLY0102	Sp LH	38.41	0.06	2.29	0.33	7.79	0.12	33.08	0.24	5.29	0.14	0.01	12.46	100.22	0.88
D70-75	HLY0102	Sp LH	37.43	0.04	2.15	0.34	7.32	0.11	32.96	0.24	5.41	0.12	0.01	14.89	101.03	0.89
D70-91	HLY0102	Sp LH	40.16	0.06	2.75	0.41	8.09	0.12	34.25	0.24	2.45	0.05	0.01	11.45	100.05	0.88
238-2-i	PS66	Sp LH	43.68	0.05	1.90	0.38	9.23	0.13	43.28	0.31	1.83	0.08	0.01	−0.34	100.52	0.89
238-2-r	PS66		43.25	0.05	2.07	0.43	9.95	0.14	41.91	0.31	2.17	0.05	0.00	−0.01	100.33	0.88
238-4-i	PS66	Sp LH	44.17	0.05	2.15	0.41	9.03	0.13	42.21	0.31	2.32	0.05	0.00	−0.27	100.54	0.89
238-4-r	PS66		41.76	0.05	2.51	0.48	9.89	0.14	40.00	0.29	2.56	0.06	0.01	2.95	100.72	0.88
238-5-i	PS66	Pl LH	44.25	0.09	3.04	0.39	9.09	0.13	40.31	0.28	2.91	0.08	0.01	−0.11	100.45	0.89
238-7-i	PS66	Sp LH	44.05	0.06	2.54	0.39	9.02	0.13	41.19	0.28	2.40	0.08	0.00	−0.09	100.05	0.89
238-7-r	PS66		43.87	0.06	2.59	0.40	9.31	0.13	40.81	0.30	2.65	0.07	0.00	0.01	100.20	0.89
238-9-i	PS66	Sp LH	44.38	0.06	2.60	0.40	9.17	0.13	41.16	0.29	2.39	0.06	0.00	−0.11	100.54	0.89
238-9-r	PS66		44.16	0.07	2.82	0.43	9.61	0.14	39.69	0.29	2.96	0.09	0.00	0.28	100.55	0.88
238-11-i	PS66	Sp LH	43.65	0.05	2.38	0.40	8.86	0.13	40.54	0.29	2.22	0.07	0.00	1.18	99.78	0.89
238-11-r	PS66		43.84	0.05	2.59	0.44	9.22	0.14	39.68	0.28	2.16	0.06	0.01	1.74	100.20	0.89
238-18-i	PS66	Sp LH	44.89	0.06	2.51	0.38	8.77	0.13	41.16	0.29	2.07	0.05	0.00	0.01	100.32	0.89
238-18-r	PS66		44.36	0.06	2.81	0.42	9.08	0.13	39.13	0.28	3.00	0.10	0.01	0.85	100.26	0.89
238-22-i	PS66	Sp HZ	43.13	0.04	1.57	0.47	8.66	0.12	44.21	0.32	1.19	0.03	0.00	−0.21	99.53	0.90
238-22-r	PS66		42.58	0.04	1.58	0.46	9.48	0.13	43.67	0.32	1.28	0.04	0.00	0.24	99.85	0.89
238-35-i	PS66	Sp LH	44.58	0.05	2.25	0.42	8.96	0.13	42.02	0.30	2.14	0.04	0.00	−0.31	100.57	0.89
238-35-r	PS66		44.05	0.05	2.33	0.45	9.76	0.14	41.50	0.30	2.10	0.05	0.00	−0.08	100.67	0.88
238-39-i	PS66	Sp LH	44.15	0.05	2.21	0.41	8.97	0.13	41.86	0.30	2.08	0.05	0.00	−0.25	99.96	0.89
238-39-r	PS66		43.30	0.05	2.30	0.44	9.67	0.14	40.65	0.30	2.26	0.06	0.00	0.19	99.38	0.88
238-49-i	PS66	Sp LH	43.28	0.04	2.16	0.38	9.04	0.13	41.64	0.30	1.96	0.07	0.01	1.14	100.15	0.89
238-49-r	PS66		42.88	0.05	2.42	0.42	9.13	0.13	39.67	0.28	2.90	0.08	0.01	1.18	99.16	0.89

Sp LH = spinel lherzolite; Pl LH = plagioclase lherzolite; Sp HZ = spinel harzburgite; FeOt = total FeO; LOI = loss on ignition; Mg# = molar Mg/(Mg+Fe); i = fresh interior; r = weathered rim.

has been interpreted as secondary sulfides added from percolating melts (Alard et al., 2000; Seyler et al., 2001; Luguet et al., 2003).

3. Methods

Major element concentrations were determined on glass with a Phillips PW 1404 X-ray Fluorescence (XRF) spectrometer at the University of Mainz. Sulfide major element compositions were analyzed on a JEOL JXA-8200 electron probe microanalyser (EPMA) at the Max-Planck Institute for Chemistry (MPI), Mainz, using an acceleration potential of 20 kV, a beam current of 20 nA and a beam diameter of 3 μm. Only sulfides in fresh PS66-238 samples were measured for major element compositions, whereas those in D70 serpentinites were not. Whole-rock sulfur abundances were determined with a carbon-sulfur analyzer CSA (carbon-sulfur analyzer) 50003 (Leybold–Heraeus) at MPI. From each sample (100–200 mg powder) three or four duplicates were measured, and the relative 2σ error of the duplicates is on average 25% at S-concentration levels of 50–100 μg/g. The sulfur content of all Gakkel peridotites is far higher than the detection limit (10 ppm).

HSE were analyzed by isotope dilution at MPI, Mainz. Detailed analytical procedures have been previously described by Büchl et al. (2002) and Liu et al. (2008). Up to 2 g powders, together with Re–Os and HSE isotope tracers (^{185}Re, ^{190}Os, ^{101}Ru, ^{106}Pd, ^{191}Ir and ^{198}Pt) and mixed acids (3 ml 12N HCl and 7 ml 16N HNO_3), were digested in a high-pressure asher (HPA-S) at 100 bar and 300 °C for 16 h. Then, HSE were separated from the whole rock matrix using the procedure described by Brügmann et al. (1999). Os was extracted from the sample solution by solvent extraction into liquid bromine and further purified by micro-distillation used the method described by Birck et al. (1997). Afterwards, Ru, Pd, Re, Ir and Pt were sequentially separated from the solution by using anion exchange columns, applying a technique modified after Rehkämper and Halliday (1997).

Osmium concentrations and isotopes were measured by N-TIMS on a Finnigan MAT-262 instrument. Details are given in Liu et al. (2008). The concentrations of other HSE were measured on a Nu Plasma MC-ICPMS, which allows measurements by static multi-collection and has the advantage that fractionation corrections are done by internal normalization or by external correction using an admixed element of similar mass. External standards were added for the mass-fractionation correction, i.e., Ir added for Re, Mo for Ru, Ag for Pd, and Os for Ir + Pt. Blank contributions are negligible because all samples have at least 20 times higher concentrations compared with the average blank compositions. Repeated digestions of fresh aliquots of the ultramafic rock standard UB-N indicate a reproducibility of 10% for the HSE concentrations (Büchl et al., 2002). The reproducibility of the concentrations, based on three duplicate analyses of samples from the present study, is 11% for Os, 3% for Ir, 12% for Ru, 5% for Pt, 9% for Pd, 9% for Re. The HSE patterns themselves were reproduced very well. Thus, the elemental ratios are less affected, although the analytical uncertainty sometimes is relatively high. The latter might reflect the heterogeneous distribution of the HSE on a small scale, the so-called 'nugget effect'.

4. Results

Whole-rock major elements of all samples are shown in Table 1. The D70 samples have lower MgO contents compared to the PS66-238 fresh peridotites, which reflect the loss of Mg during seawater alteration of abyssal peridotites on the seafloor (Snow and Dick, 1995). The common slightly lower MgO contents of the altered rims of the PS66-238 samples compared to their corresponding fresh cores are consistent with this hypothesis as well. The D70 samples also have

Table 2
Major element compositions of representative sulfides in the PS66-238 samples.

Sample	PS66-238-2							PS66-238-4			PS66-238-5				
Assemblage	Pn		Po	Cp	Pn+Po	Pn+Cp	Pn+Cp	Pn		Po	Pn		Po		Cu-rich Po
Type	inter	in	inter	in	inter	inter	in	in	inter	inter	in	inter	in	inter	inter
Fe	32.27	33.05	62.29	29.10	46.04	36.62	34.49	33.64	34.62	62.22	38.09	36.93	61.91	62.12	54.20
Ni	33.14	32.84	0.10	0.08	15.08	26.64	28.90	31.94	30.47	0.07	26.76	28.64	0.29	0.19	0.16
Co	0.47	0.23	0.05	0.03	0.38	0.58	0.58	0.29	0.36	0.05	0.51	0.37	0.06	0.06	0.05
Cu	0.03	0.01	0.05	33.92	0.29	1.14	1.14	0.19	0.25	0.03	0.07	0.08	0.08	0.31	7.98
S	32.18	32.07	35.24	33.56	35.86	31.91	31.61	32.58	32.51	35.98	32.19	32.18	34.98	35.34	36.83
Si	0.36	0.25	0.26	0.39	0.29	0.23	0.35	0.31	0.35	0.30	0.42	0.34	0.33	0.26	0.27
Total	98.59	98.55	98.09	97.12	97.96	97.24	97.24	99.11	98.66	98.74	98.17	98.67	97.79	98.39	99.64

Sample	PS66-238-7					PS66-238-9			PS66-238-11		PS66-238-18		
Assemblage	Pn		Cu-rich Pn	Pn+Cp	Po	Pn		Po	Pn	Cu-rich Pn	Pn		Cu-rich Pn
Type	in	inter	inter	inter	in	in	inter	inter	inter	in	in.	inter	inter
Fe	37.92	38.48	38.78	24.42	63.08	39.25	39.47	61.31	43.85	40.29	37.45	42.20	39.43
Ni	26.24	27.07	24.51	26.87	0.01	26.00	25.80	0.05	21.18	20.62	27.51	22.46	22.81
Co	0.52	0.45	0.47	0.31	0.05	0.49	0.55	0.05	0.45	0.43	0.36	0.45	0.39
Cu	0.83	0.05	1.27	13.65	0.00	0.00	0.14	0.24	0.07	1.86	0.24	0.24	2.33
S	32.16	32.48	32.48	32.46	35.01	32.46	32.55	36.57	32.90	31.12	32.44	32.75	32.20
Si	0.41	0.32	0.44	0.34	0.31	0.34	0.28	0.24	0.27	0.91	0.33	0.37	0.63
Total	98.23	98.99	98.07	98.15	98.59	98.62	98.93	98.56	98.85	95.30	98.45	98.58	97.85

Sample	PS66-238-22			PS66-238-35			PS66-238-39				PS66-238-49			
Assemblage	Pn		Po	Pn		Pn+Cp+Po	Pn		Cu-rich Pn	Po	Pn		Cu-rich Pn	Cu-rich Pn
Type	in	inter	inter	in	inter	in	in	inter	inter	inter	in	inter	inter	in
Fe	33.67	34.52	60.17	32.55	30.64	47.25	32.52	32.26	37.73	61.07	38.94	41.57	38.66	38.35
Ni	31.43	30.54	0.13	33.11	34.43	14.52	32.91	33.52	22.89	0.03	26.21	23.96	20.51	22.53
Co	0.34	0.41	0.05	0.39	0.53	0.10	0.54	0.20	0.13	0.04	0.48	0.45	0.44	0.45
Cu	0.46	0.18	0.13	0.08	0.60	1.38	0.06	0.00	3.29	0.06	0.06	0.07	5.71	3.95
S	32.21	32.14	36.18	32.21	32.25	35.05	32.56	32.32	33.43	36.76	32.43	32.39	33.38	32.90
Si	0.32	0.35	0.25	0.25	0.37	0.29	0.33	0.25	0.42	0.29	0.29	0.26	0.31	0.36
Total	98.57	98.29	97.01	98.73	98.95	98.75	98.99	98.65	98.02	98.36	98.49	98.86	99.09	98.61

1: inter = interstitial; in = inclusion.
2: Pn = Pentlandite; Po = Pyrrhotite; Cp = Chalcopyrite.

Table 3
HSE and sulfur contents of Gakkel ridge abyssal peridotites.

Sample	Lithology	Os (ppb)	Ir (ppb)	Ru (ppb)	Pt (ppb)	Pd (ppb)	Re (ppb)	$^{187}Os/^{188}Os$	S (ppm)	
									avg.	1σ
D70-91	Sp LH	2.07	1.72	4.65	5.36	5.17	0.13	0.1292 ± 3	549	191
D70-58	Sp LH	1.72	1.14	4.07	3.78	3.21	0.05	0.1301 ± 3	288	60
Replicate		2.85	1.13	5.34	4.18	3.50	0.05	0.1306 ± 2		
D70-56	Sp LH	3.38	3.33	7.37	7.76	3.03	0.25	0.1261 ± 2	766	145
D70-75	Sp LH	3.01	3.11	6.28	6.92	2.30	0.14	0.1277 ± 3	466	42
D70-62	Sp HZ	4.05	3.95	5.28	2.66	0.74	0.16	0.1149 ± 2	478	74
D70-64	Sp LH	2.14	2.42	3.79	3.44	2.87	0.29	0.1226 ± 3	582	75
D70-73	Sp LH	3.30	3.17	6.72	7.47	2.99	0.29	0.1285 ± 4	407	89
238-2-i	Sp LH	4.34	4.35	7.94	8.83	8.45	0.22	0.1266 ± 2	72	5
238-4-i	Sp LH	4.53	4.55	8.43	7.99	8.59	0.36	0.1286 ± 2	93	16
238-4-r		4.21	4.71	8.41	7.97	7.20	0.30	0.1296 ± 2	102	9
238-5-i	Pl LH	3.90	3.77	6.69	6.83	6.22	0.32	0.1271 ± 2	137	12
238-7-i	Sp LH	4.66	4.45	8.18	8.75	6.95	0.30	0.1263 ± 3	120	14
238-9-i	Sp LH	4.56	4.42	8.30	7.43	7.21	0.31	0.1261 ± 2	127	15
238-11-i	Sp LH	3.80	3.47	7.00	6.13	5.10	0.22	0.1240 ± 2	114	6
Replicate		3.97	3.62	6.98	6.04	4.70	0.25	0.1238 ± 3		
238-11-r	Sp LH	5.57	4.47	9.59	8.95	4.13	0.22	0.1247 ± 3	114	15
Replicate		4.69	4.29	8.64	9.47	4.67	0.24	0.1248 ± 3		
238-18-i	Sp LH	5.39	5.16	8.47	8.08	5.99	0.34	0.1225 ± 2	163	3
238-22-i	Sp HZ	6.71	5.30	10.70	5.56	4.58	0.23	0.1139 ± 2	96	16
238-22-r		6.58	5.46	10.86	7.10	3.55	0.13	0.1165 ± 2	75	9
238-35-i	Sp LH	4.71	4.66	7.99	8.50	7.57	0.28	0.1279 ± 2	87	12
238-39-i	Sp LH	5.46	5.09	9.34	9.59	7.91	0.29	0.1274 ± 2	77	6
238-39-r		4.30	4.56	8.22	8.06	6.97	0.29	0.1278 ± 2	100	10
238-49-i	Sp LH	4.44	3.72	7.85	7.15	6.02	0.22	0.1237 ± 2	104	9
238-49-r		4.36	3.87	7.91	7.70	3.82	0.24	0.1252 ± 2	110	18

-i: fresh interior; -r: weathered rim.
Sp LH = Spinel Lherzolite; Sp HZ = Spinel Harzburgite; Pl LH = Plagioclase Lherzolite.
avg = average; σ = standard deviation.
Re and Os data from Liu et al. (2008).

higher contents of Na_2O and CaO than the PS66-238 samples, whereas the fresh cores of the PS66-238 samples have very low Na_2O contents of (0.03–0.08%). This suggests that both Ca and Na were added to D70 samples during seawater alteration. Both D70 and PS66-238 samples have very low TiO_2 abundances (0.03–0.09%).

Representative compositions of different sulfides in the fresh PS66-238 samples are listed in Table 2. Sulfides in all samples are mainly composed of pentlandite and pyrrhotite. Secondary Cu-rich sulfides commonly reported in previous studies (Luguet et al., 2003; Alard et al., 2005) are seldom observed in the "fresh" Gakkel abyssal peridotites, and chalcopyrite grains have only been discovered in one sample (PS66-238-2). Previous studies observe sulfides in mantle peridotites that show differences in their major elements according to whether they are found on grain boundaries or grain interiors (Alard et al., 2005; Lorand and Gregoire, 2006). By contrast, no significant difference among these different types of sulfides is observed in the PS66-238 samples.

The fresh dredge PS66-238 samples have much lower bulk-rock sulfur contents relative to the D70 serpentinites (Table 3). Furthermore, sulfur contents of the PS66-238 samples (72–163 ppm) are also lower than in the primitive mantle (ca. 250 ppm; (McDonough and Sun, 1995)). The fresh interiors and the altered rims from the same PS66-238 samples do not have distinguishably different sulfur contents. Sulfur contents of PS66-238 samples display a weak positive correlation with their bulk Al_2O_3 contents (Fig. 2). The harzburgite 238-22 and one lherzolite (238-18) deviate from the correlation to a higher value. Compared to the PS66-238 samples, D70 serpentinites have much higher sulfur contents (288–766 ppm), probably reflecting the addition of sulfur from seawater to the serpentinites (Alt and Shanks, 1998). Their sulfur contents correlate neither with bulk Al_2O_3 contents nor with HSE ratios.

The HSE concentrations of both D70 and PS66-238 samples are listed in Table 3. Notably, the D70 serpentinites have lower HSE concentrations than the PS66-238 samples (Fig. 3), even after recalculation by their LOI. The HSE abundances of the D70 samples are less than 0.01 × CI (CI chondrites) (Fig. 3a). All six D70 lherzolites but D70-58 have chondritic Os/Ir ratios. Sample D70-58 has the lowest Ir and Re contents and thus gives suprachondritic PGE/Ir ratios. Replicate analyses of this sample show that the concentrations of Ir, Re, and Pd are highly reproducible, whereas both Os and Ru concentrations are variable. Thus, low concentrations of both Ir and Re in this sample are not likely to be an analytical artifact. Lherzolite D70-91 also has suprachondritic PGE/Ir ratios. Ru/Ir ratios in all lherzolites are suprachondritic, whereas Re/Ir ratios are commonly subchondritic. The harzburgite D70-62 has a fractionated HSE pattern with higher IPGE but lower PPGE, thus giving lower $(Pt/Ir)_n$, $(Pd/Ir)_n$ and $(Re/Ir)_n$ (n: CI-chondrite normalized; (Horan et al., 2003)) ratios of 0.31, 0.15 and 0.48, respectively.

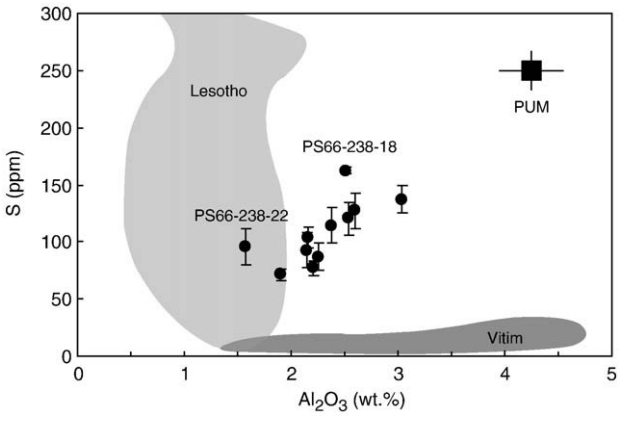

Fig. 2. Diagram of whole-rock sulfur content versus bulk Al_2O_3 content. Slightly positive correlation exists among the fresh interiors of PS66-238 samples. The harzburgite (PS66-238-22) deviates from the correlation to a relatively higher value. One lherzolite (PS66-238-18) also deviates from the correlation to a higher value. The data of Lesotho (Pearson et al., 2004) and Vitim (Ionov et al., 1992) mantle xenoliths are shown for comparison. The PUM data are from McDonough and Sun (1995).

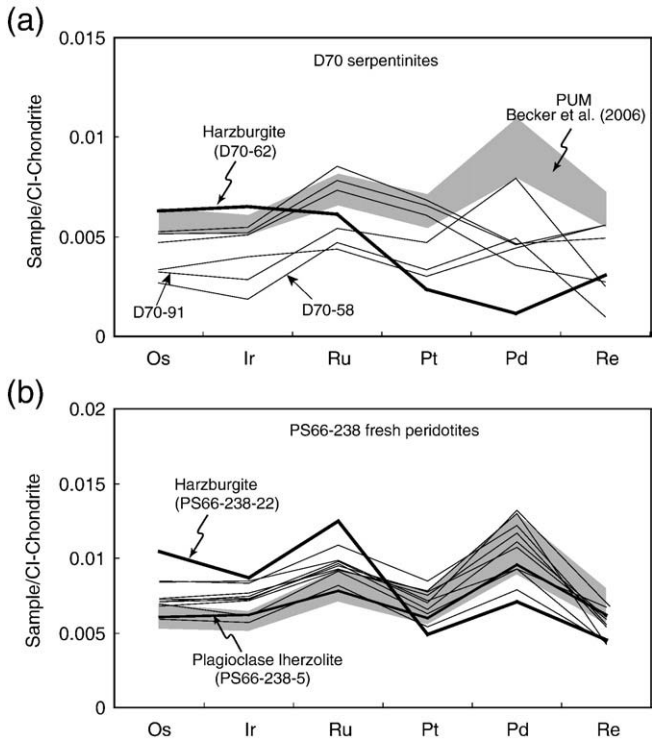

Fig. 3. Diagrams of HSE patterns of (a) HLY0102-D70 and (b) PS66-238 samples. (a) D70 lherzolites have consistent IPGE patterns but variable PPGE and Re patterns. (b) All PS66-238 lherzolites have consistent patterns. Both harzburgite (PS66-238-22) and plagioclase lherzolite (PS66-238-5) have fractionated HSE patterns. The harzburgite has higher contents of I-PGEs relative to P-PGEs and Re, whereas the plagioclase lherzolite has slightly higher Pd and Re contents. The HSE pattern of the D70 harzburgite (D70-62) is similar to that of PS66-238 harzburgite, i.e., higher contents of IPGE and lower PPGE and Re. CI-chondrite normalizing values are from Horan et al. (2003).

The PS66-238 fresh peridotites have higher platinum group elements (PGE: Os, Ir, Ru, Pt and Pd) but lower Re abundances relative to the primitive mantle (McDonough and Sun, 1995), and their PGE patterns are consistent than those of D70 samples. All fresh interiors of lherzolites have chondritic Os/Ir, supra-chondritic (Ru, Pd)/Ir, but sub-chondritic (Pt, Re)/Ir ratios (Fig. 3b). The harzburgite (PS66-238-22) has fractionated HSE pattern with supra-chondritic IPGE (Os, Ir, and Ru) but sub-chondritic PPGE (Pt and Pd) and Re. Three of the five analyzed weathered rims have similar IPGE abundances to their interiors. Two rims have higher (PS66-238-11) and lower (PS66-238-39) contents than their interiors, respectively. All weathered rims have higher Pd contents than their corresponding fresh interiors. Only two samples (PS66-238-4 and PS66-238-22) have lower Re contents in their fresh interiors than their weathered rims, whereas other three samples have similar Re contents between interiors and rims.

5. Discussion

5.1. Effects of seawater alteration

Abyssal peridotites are commonly subjected to pervasive alteration during their exposure to circulating fluids and seawater at or below the seafloor. Therefore, effects of alteration on the HSE compositions of abyssal peridotites should be evaluated before using HSE data to discuss the processes in the oceanic mantle. Seawater alteration of abyssal peridotites is a complicated process, including both serpentinization (~500 °C–0 °C) and weathering (~0 °C) processes, and could take place under a range of temperatures and redox conditions at different stages (Bach et al., 2004; Snow and Dick, 1995). The behaviors of the HSE during seawater alteration of abyssal peridotites remain poorly constrained. It has been suggested that platinum-group elements (PGE) are stable during serpentinization processes because they are all extremely unreactive in a reducing environment (Snow and Schmidt, 1998). Serpentinization of peridotites has thus been thought to be without significant effect on HSE relative abundances other than diluting total HSE contents (Lorand et al., 1993), owing to a volume increase caused by serpentinization of silicate phases (Snow and Schmidt, 1998). Unlike serpentinization, seawater weathering processes occur under an oxidizing environment, and thus, could potentially affect the HSE compositions of abyssal peridotites (Snow and Schmidt, 1998). Decrease of Pd abundance has been observed in altered abyssal peridotites, indicating its mobile character during oxidizing seafloor alteration (Luguet et al., 2003).

Fresh peridotites with weathered rinds from Gakkel Ridge provide an opportunity to evaluate the effects of seawater alteration on the HSE composition of abyssal peridotites. In the five analyzed PS66-238 samples, Os, Ir, Ru and Pt show no systematic difference between the weathered rims and the fresh interiors (Fig. 4), which suggests that these elements are not affected by seawater alteration. Therefore, IPGE are immobile and preferentially retained in the serpentinites during alteration, possibly because the magmatic sulfides were still preserved through seafloor alteration. Consistent with the previous conclusion that Pd tends to be mobile during seafloor weathering (Luguet et al., 2003), the altered rims of the five PS66-238 samples have Pd contents lower than those of their interiors (Fig. 4). Furthermore, the analyzed fresh interiors have Re contents either higher than or similar to their corresponding altered rims. This suggests that Re also tends to be mobile during seawater alteration of abyssal peridotites. The following discussion will be focused only on the HSE data of the fresh interiors of the PS66-238 samples.

5.2. Fractionation of HSE during partial melting

It has been widely demonstrated that incongruent melting of sulfides in mantle peridotites produces Cu–Ni-rich sulfide melt, and leaves residual monosulfide solid solution (Mss) in the peridotite residues (Alard et al., 2000; Luguet et al., 2003; Bockrath et al., 2004; Peregoedova et al., 2004; Ballhaus et al., 2006). The refractory Mss concentrates Os, Ir and Ru, whereas the Cu–Ni-rich sulfides are

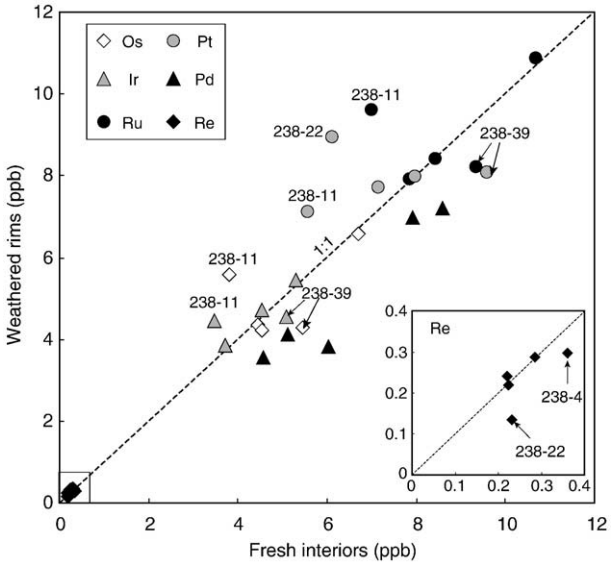

Fig. 4. Comparison of HSE data between the fresh interiors and the weathered rims. Three of the five analyzed weathered rims have similar IPGE abundances as their interiors. Sample 238-11 has higher contents of IPGE in its weathered rim than its fresh interior, but vice versa in sample 238-39. All weathered rims have higher Pd contents than their corresponding fresh interiors. Only two samples (PS66-238-4 and PS66-238-22) have lower Re contents in their fresh interiors than their weathered rims, whereas other three samples have similar Re contents between interiors and rims.

enriched in Pt, Pd and Re (Alard et al., 2000; Bockrath et al., 2004; Ballhaus et al., 2006). The Cu–Ni-rich sulfide melt could be physically removed along with the basaltic melt, which would result in the depletion of Pt, Pd and Re in the peridotite residues (Ballhaus et al., 2006). In this physical process, fractionation of PGE in mantle peridotites is not controlled by their sulfide/silicate partition coefficients but by their Cu–Ni-rich sulfide/Mss partition coefficients.

By the use of the Cr# [=Cr/(Cr+Al)] of spinel (Dick and Bullen, 1984; Hellebrand et al., 2001), the PS66-238 spinel lherzolites can be estimated to have experienced 5–8% silicate partial melting. As shown in Fig. 3b, they display consistent HSE patterns. All spinel lherzolites have uniform ratios of both Os/Ir and Ru/Ir along with the melt depletion index (e.g., bulk Al_2O_3 content) (Fig. 5a and b), indicating the compatible nature of Os, Ir and Ru during partial melting. The horizontal relationship between Pt/Ir and the degree of partial melting (F) shown among all lherzolites (Fig. 6a), suggests that Pt also behaves as a compatible element. Furthermore, all lherzolites have uniform Pt/Pd values for a wide range of bulk Al_2O_3 contents, indicating that Pd did not fractionate from Pt and the IPGE (Fig. 5c). The lack of fractionation of PGE in the PS66-238 spinel lherzolites suggests that they were not significantly affected by sulfide melt removal during partial melting. By contrast, the harzburgite PS66-238-22 was subjected a higher degree of partial melting (ca. 12%) and displays a fractionated HSE pattern, with depletion of PPGE and Re relative to IPGE (Fig. 3b). Modeling results suggest that the sulfides in mantle peridotites would be totally consumed by about 12% partial melting (Luguet et al., 2003). Therefore, depletion of Pt and Pd in the harzburgite might reflect the total consumption of sulfide in this sample.

To illustrate the fractionation of PGE in the peridotites during melting of mantle sulfides, we modeled the variations of both Pt/Ir and Pd/Ir ratios (Fig. 6), using the method of previous studies (Lorand et al., 1999; Luguet et al., 2003). Here we assume that the DMM contained 150 ppm S before melting and the solubility of S in the basaltic melts is 1000 ppm. Other details and parameters are given in Fig. 6. The result indicates that D_{Pt} must vary from <2000 to 5000 to account for the subchondritic Pt/Ir ratios in PS66-238 samples (Fig. 6a), which is consistent with previous experimental work (Stone et al., 1990; Fleet et al., 1991). Considering the large variation of Pd/Ir ratios among the different chondrites (Horan et al., 2003), both the CI-chondritic Pd/Ir ratio (1.3) and the higher Pd/Ir value similar to EH4 enstatite chondrites (1.6, e.g., Rehkämper et al. (1999)) were taken for modeling. No matter which Pd/Ir ratio is chosen (Fig. 6b), a very low D_{Pd} (ca. 2000) value is required to reproduce the Pd content in the harzburgite, which is 5 to 10 times lower than D_{Ir}. This conflicts with previous experimental results (Fleet et al., 1991; Fleet et al., 1999), in which quite similar values for D_{Ir} and D_{Pd} were obtained. Depletion of Pd in the harzburgite thus cannot be explained by equilibrium partitioning between sulfide and silicate melt, nor by congruent melting of sulfides along the peridotites solidus. It most likely reflects instead the incongruent melting of mantle sulfide and the drainage of the Cu–Ni-rich sulfide melt by the basaltic melt.

Good positive correlations between Re/Os and bulk Al_2O_3 ratios shown by all but one lherzolite suggest that Re was incompatible even

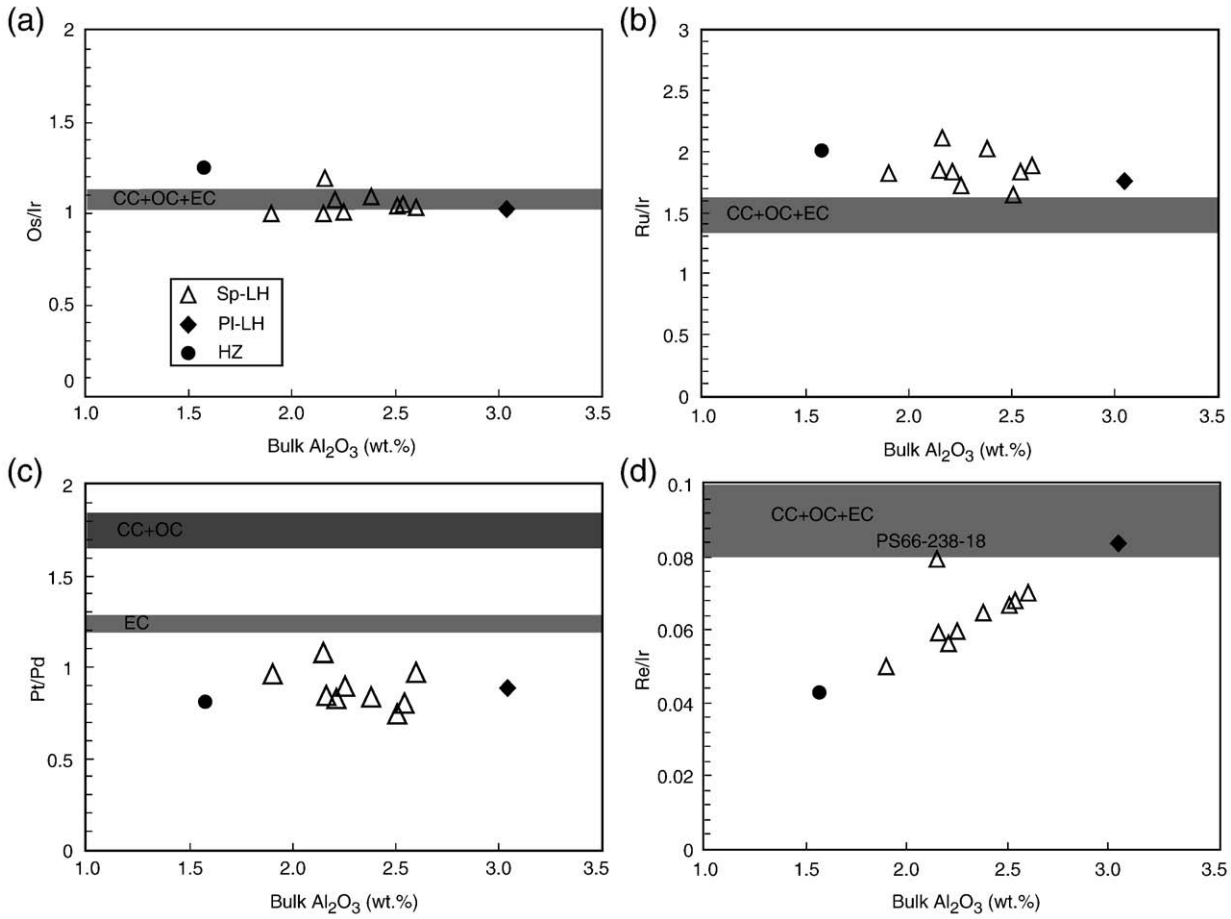

Fig. 5. PGE ratios versus bulk Al_2O_3 contents. (a–b) Both Os/Ir and Ru/Ir ratios of all PS66-238 samples display horizontal lines along the variation of bulk Al_2O_3 contents. This suggests Os, Ir and Ru behave compatibly during low to moderate degree of partial melting (up to 12%). (c) Pt/Pd ratios of all PS66-238 samples show a flat line with bulk Al_2O_3 contents, reflecting these two elements were not fractionated during partial melting. (d) All PS66-238 samples but one lherzolite (PS66-238-18) show good positive relationship between Re/Ir ratio and bulk Al_2O_3 content, which suggests Re is similar to Al during partial melting and also melt refertilization. CC = Carbonaceous Chondrite; OC = Ordinary Chondrite; EC = Enstatite Chondrite. Sp-LH = spinel lherzolite; Pl-LH = plagioclase lherzolite; HZ = harburgite.

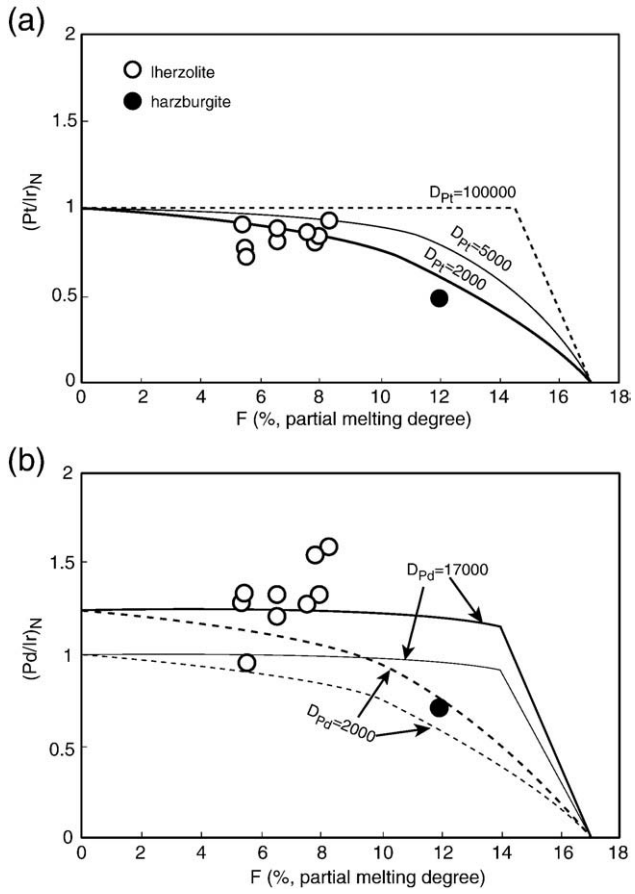

Fig. 6. Modeling the variations of $(Pt/Ir)_N$ (a) and $(Pd/Ir)_N$ ratios (b) in the Gakkel Ridge abyssal peridotites during partial melting. N = CI-chondrite normalized (Jochum, 1996). Two Pd/Ir values were chosen for DMM sources, one CI-chondritic, and the other similar to EH4 enstatite chondrites Horan et al. (2003). A constant sulfide melt-silicate melt partition coefficient was selected for Ir from Fleet et al. (1999). Different partition coefficients of Pt and Pd marked along the curves were used for modeling. Note that Pd/Ir ratios in some lherzolites are even higher than the values of EH4 enstatite chondrites. Other details are given in the text.

at low degrees of partial melting (Fig. 5d). This is consistent with previous inferences that Re behaves as a moderately incompatible element with a bulk partition coefficient similar to that of aluminum (Reisberg and Lorand, 1995; Shirey and Walker, 1998). This might be because the budget of Re in mantle peridotites is mainly controlled by silicates and spinels (Luguet et al., 2007).

5.3. PS66-238 spinel lherzolites: pristine mantle peridotites or secondary rocks resulting from refertilization of harzburgite?

Based on the structural and geochemical evidence, Le Roux et al. (2007) have recently demonstrated that some lherzolites from the Lherz massif do not represent pristine mantle rocks but instead are secondary rocks formed by refertilization of harzburgites. The authors suggested that most lherzolite massifs represent secondary (refertilized) rather than pristine mantle. Furthermore, it has been shown that Re–Os systematics in some massif lherzolites reflect the refertilization of ancient refractory peridotites with enriched melts (van Acken et al., 2008). Therefore, application of orogenic lherzolites to infer the composition of the PUM (Meisel et al., 2001; Becker et al., 2006) should be approached with caution (Lorand et al., 2008). Clinopyroxene trace element compositions of lherzolites from PS66-238 suggest that they have been refertilized by late melts after low degrees of melt extraction (Liu et al., 2008), which is also supported by the occurrence of plagioclase lherzolite (PS66-238-5). Therefore, it is important to assess whether the PS66-238 lherzolites represent fertile pristine mantle rocks or not.

The following three lines of evidence suggest that the PS66-238 lherzolites were not transformed from harzburgites through melt refertilization. First, the Gakkel Ridge is the slowest spreading mid-ocean ridge in the world, beneath which the abyssal peridotites should be subjected to low degrees of partial melting. Particularly, the PS66-238 samples were collected from the segment with the weakest magmatism, around which no basalt but only peridotites have been recovered (see the Fig. 1 in Liu et al. (2008)). Therefore, the large amounts of melt required to produce lherzolite through refertilization of harzburgite are unlikely to be present in this area.

Second, the lherzolites have only slightly higher contents of both Na_2O (0.04–0.08%) and TiO_2 (0.05–0.09%) compared to those of the harzburgite PS66-238-22 with 0.03% and 0.04%, respectively. Assuming the refertilizing melts have N-MORB-like compositions with 2% Na_2O and 1% TiO_2, the amount of melts required should be no larger than 5%. This precludes the formation of lherzolites through impregnation of large amounts of melt (10%) into harzburgite (Le Roux et al., 2007).

Third, their Re–Os isotopes argue against the transformation from harzburgites. The harzburgite PS66-238-22 has higher Os abundance but lower $^{187}Os/^{188}Os$ ratio compared to the lherzolites. To increase the $^{187}Os/^{188}Os$ ratio, radiogenic Os would have to be added into the harzburgite along with refertilizing silicate melts, because percolation of pure sulfide melt has been argued against in the PS66-238 samples (Liu et al., 2008). The Os content of harzburgite could be reduced either by addition of large amounts of silicate melt through a dilution effect or by removing the primitive unradiogenic Os. The former process is impossible because an unrealistically large volume of melt (>15%) is required to decrease the Os concentration from 6.71 ppb in the harzburgite to 5.46 ppb in PS66-238-39, which has the highest Os concentration among the lherzolites. Removal of primitive unradiogenic Os along with addition of radiogenic Os, however, commonly takes place at high melt/rock ratios and open systems, such as during the formation of dunite (Büchl et al., 2002), rather than during melt refertilization processes, which take place at lower melt/rock ratios.

5.4. Non-chondritic HSE of spinel lherzolites from Gakkel Ridge: implications for the HSE composition of the PUM

Notably, both Ru and Pd in all spinel lherzolites from Gakkel ridge are enriched relative to Ir and Os, that is, they have suprachondritic Ru/Ir and Pd/Ir ratios. Rhenium and Pt abundances are not enhanced (Fig. 3b). Suprachondritic Ru/Ir ratios have been widely reported in mantle peridotites from different tectonic settings (Rehkämper et al., 1997; Snow and Schmidt, 1998; Schmidt et al., 2000; Pearson et al., 2004), and has been suggested to be an indigenous characteristic of a large fraction, if not of the whole of the upper mantle (Palme and O'Neill, 2004). Many bulk rock samples of fertile lherzolites also show enrichment of Pd over Ir when normalized to carbonaceous chondrites or even enstatite chondrites (Pattou et al., 1996; Snow and Schmidt, 1998; Lorand et al., 1999; Rehkämper et al., 1999; Schmidt et al., 2000; Lorand et al., 2000; Lee, 2002; Luguet et al., 2003; Pearson et al., 2004; Becker et al., 2006). However, it has been highly debated whether this results from secondary processes (Rehkämper et al., 1999; Schmidt et al., 2000; Morgan et al., 2001; Luguet et al., 2003; Pearson et al., 2004), or is an indigenous feature of the Earth's upper mantle (Becker et al., 2006).

Melt refertilization and metasomatism are the two secondary igneous processes occurring in mantle peridotites 'en route' to the Earth's surface. New mineral phases would be formed in a metasomatic process through the reaction of melt with phases in the peridotite (Kelemen et al., 1992), whereas a melt refertilization process would lead the originally refractory peridotite (e.g., harzburgite) to become fertile peridotite (e.g., lherzolite) (Elthon, 1992). Both

processes are capable of changing the HSE composition of mantle peridotites (Rehkämper et al., 1999; Saal et al., 2001; Büchl et al., 2002; Luguet et al., 2003; Pearson et al., 2004), because secondary igneous sulfides could be segregated from the melts into mantle peridotites together with other silicate minerals (Seyler et al., 2001). Suprachondritic Pd/Ir ratios in the PS66-238 samples cannot be attributed only to the addition of silicate melts. As discussed above, addition of large amounts of melt is unlikely in PS66-238 lherzolites because of their low contents of both Na_2O and TiO_2. The peridotite-melt partition coefficient of Re is lower than that of Pd. If melt refertilization were responsible for Pd enhancement in the lherzolites, Re would be enriched relative to Pd or Pt, which it is not.

By comparison, percolation of sulfide melt would be more efficient than silicate melt in increasing the Pd/Ir ratios of mantle peridotites. Rehkämper et al. (1999) first proposed the addition of secondary sulfides to explain suprachondritic Pd/Ir ratios observed in some mantle peridotites. They implied that the HSE budget of mantle peridotites reflects the physical mixing of both residual and secondary sulfides. In-situ study of base-metal sulfides provides further support to this interpretation. Relative to sulfides enclosed in olivine, interstitial sulfides in mantle peridotites are generally enriched in incompatible PGEs (i.e., Pd and Re) on one hand; and also have suprachondritic $^{187}Os/^{188}Os$ ratios on the other hand (Alard et al., 2000; Alard et al., 2005). Modeling results showed that addition of 50–100 ppm sulfur in the form of secondary sulfide is enough to account for the suprachondritic Pd/Ir observed in some mantle peridotites (Rehkämper et al., 1999; Luguet et al., 2003).

Some sulfides in Gakkel abyssal peridotites do bear both compositional and textural evidence supporting for their magmatic origin. Chalcopyrite and Cu–Ni-rich sulfides interstitial among silicate minerals have been observed in some samples. Especially, association of some small sulfides with tiny cpx (cpx_2) and spinel (sp_2) occur in some Gakkel samples (Fig. 1c, f). Such textures have been reported in abyssal peridotites and ophiolitic peridotites, which were commonly attributed to crystallization of magmatic sulfides from small refertilizing melt fractions trapped within the peridotites (Seyler et al., 2001; Luguet et al., 2003; Luguet et al., 2004). Furthermore, sulfur contents of both PS66-238-18 and PS66-238-22 deviate from the positive Al_2O_3–S correlation to higher values, possibly reflecting the late addition of sulfides in these samples. Therefore, at least some Gakkel peridotites have been affected by late addition of magmatic sulfides.

However, suprachondritic Pd/Ir ratios in all PS66-238 lherzolites are unlikely to result from addition of metasomatic sulfides for the following reasons. The first set of reasons is petrographic: the refractory Fe–Ni-rich sulfides (i.e., pentlandite and pyrrhotite) predominate over Cu–Ni-rich sulfides and chalcopyrite in all samples. Even when they occur, the Cu–Ni-rich sulfides are very tiny in size. Sample PS66-238-4 has a suprachondritic Pd/Ir, even though no Cu-rich magmatic sulfide has been discovered in thin section. Secondly, sulfide addition process cannot account for the significantly different Pd/Ir ratios in samples with similar histories of partial melting and melt refertilization. For example, sample PS66-238-2 and PS66-238-39 have been subjected with similar degrees of melt extraction, indicated by the similar Cr# of their spinels (0.2 vs. 0.18). They also contain identical sulfur contents within error (72 vs. 77 ppm). This suggests that similar amount of sulfides were added into these two samples after melt extraction, if this process was occurred in both samples. However, the $(Pd/Ir)_N$ value of PS66-238-2 (1.93) is much higher than that of PS66-238-39 (1.43). Thirdly, addition of magmatic sulfides does not explain the S-PGE systematics. We have calculated an excess sulfur content for each sample as the measured sulfur content of the sample minus the theoretical sulfur content residual in the sample after partial melting. Magmatic sulfides have high Pd/Ir ratios compared to mantle rocks, predicting a strong positive correlation of Pd/Ir with added sulfide. In Fig. 7, models are shown assuming Pd/Ir in magmatic sulfides of 2 and 5.3, respectively. Instead of a positive correlation, there

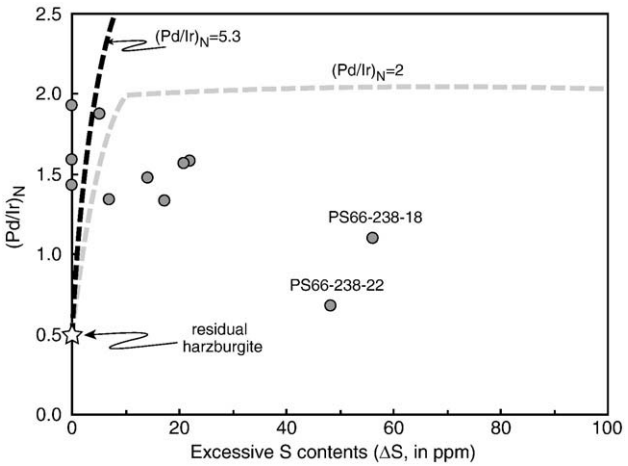

Fig. 7. Correlation between the $(Pd/Ir)_N$ ratios and the excess sulfur content (ΔS). $\Delta S = S_M - S_T$; S_M, the measured sulfur content; S_T, the theoretical values in the peridotite residues after different degrees of partial melting from a mantle source with 150 ppm S. Two samples (PS66-238-18 and PS66-238-22) with the maximum excess sulfur contents have the lowest Pd/Ir ratios. The dash lines show the modeling of addition of magmatic sulfides with different Pd/Ir ratios into a residual harzburgite, which contain 4 ppb Ir, 2.2 ppb Pd and has a $(Pd/Ir)_N$ ratio of 0.5. The black dash line represent the addition of a magmatic sulfide with 45 ppm Ir, 280 ppm Pd and a $(Pd/Ir)_N$ ratio of 5.3. The grey dash line represent the addition of a magmatic sulfide with 56 ppm Ir, 120 ppm Pd and a $(Pd/Ir)_N$ ratio of 2. Compositions of the magmatic sulfides are selected from Luguet et al. (2001).

is a rough inverse relationship between the Pd/Ir ratio and the excess sulfur content (except for the harzburgite), which essentially contradicts the contention that the suprachondritic Pd/Ir ratios in the Gakkel Ridge lherzolites result from pervasive addition of secondary magmatic sulfides (Fig. 7). The two samples (PS66-238-18 and PS66-238-22) with the maximum excess sulfur contents have the lowest Pd/Ir ratios, and (again with the exception of the harzburgite) all samples with low excess sulfur have high Pd/Ir ratios. Therefore, we conclude that suprachondritic Pd/Ir ratios in Gakkel lherzolites are not due to addition of metasomatic sulfides. Instead, similar to the suprachondritic Ru/Ir ratio, they represent an indigenous signature of the Earth's upper mantle.

The non-chondritic HSE patterns displayed by the fresh PS66-238 lherzolites, i.e., suprachondritic Ru/Ir and Pd/Ir ratios but chondritic Pt/Ir ratio, are similar to those of the PUM. The estimated composition of the PUM were inferred based on samples representative of continental lithospheric mantle, e.g., peridotite massifs and mantle xenoliths (Becker et al., 2006). This suggests that the oceanic mantle has a HSE budget similar to that of the continental lithospheric mantle. Meanwhile, unlike some samples previously used for the estimate of the PUM composition, the Gakkel lherzolites have experienced little melt refertilization. Our results thus support the conclusion that the PUM has a non-chondritic HSE budget.

6. Conclusions

Abyssal peridotites from the ultra-slow spreading Gakkel Ridge that experienced little melt extraction and late refertilization provide an opportunity to study the behaviors of the HSE during seawater alteration and partial melting, and also provide constraints on the HSE composition of the primitive upper mantle (PUM). Comparison of HSE compositions between fresh, weathered and serpentinized abyssal peridotites suggest that the HSE with the possible exception of Pd and Re are stable during seafloor alteration (i.e., serpentinization and weathering). The lherzolites from Gakkel Ridge have very low contents of both Na_2O and TiO_2, representing the pristine mantle rather than secondary refertilization mantle. They have consistent HSE patterns with suprachondritic Ru/Ir and Pd/Ir ratios. The

harzburgite has a fractionated HSE pattern with depletion in Pt, Pd and Re. This might reflect the removal of Cu–Ni-rich sulfide from the harzburgite during partial melting, perhaps through a physical draining process. The suprachondritic Pd/Ir ratios of the PS66-238 lherzolites are not due to the addition of metasomatic sulfides, although these have been discovered in some samples. Therefore, both the suprachondritic Pd/Ir ratio and the suprachondritic Ru/Ir ratio are indigenous characteristics of the upper mantle. Our conclusion is consistent with the HSE composition of the PUM estimated based on the HSE concentrations in rocks from the continental lithospheric mantle.

Acknowledgements

We thank the Captain and crew of PFS Polarstern expedition ARK XX/2 and the other participants in the AMORE 2001 expedition. This work overall was supported by the Max-Planck Institute for Chemistry and the Deutsche Forschungsgemeinschaft to J.E.S. We are indebted to Anette von der Handt, Zoran Jovanovic and Yong-Jun Gao for their help with the sample preparation and experiments. K. Zentel and J. Krause are thanked for their help in HSE and Os isotopes experiments, and Reinhard Haubold for the sulfur analysis. C.Z.L. received scholarships from both Chinese Academy of Sciences and Max-Planck Institute for Chemistry. This research was partly supported by NSFC grant (40873024) to C.Z.L. We thank R.J. Walker and A. Luguet for their constructive reviews on this manuscript and R. Carlson for the editorial handling.

References

Alard, O., Griffin, W.L., Lorand, J.P., Jackson, S.E., O'Reilly, S.Y., 2000. Non-chondritic distribution of the highly siderophile elements in mantle sulphides. Nature 407, 891–894.

Alard, O., Luguet, A., Pearson, N.J., Griffin, W.L., Lorand, J.P., Gannoun, A., Burton, K.W., O'Reilly, S.Y., 2005. In situ Os isotopes in abyssal peridotites bridge the isotopic gap between MORBs and their source mantle. Nature 436, 1005–1008.

Alt, J.C., Shanks, W.C., 1998. Sulfur in serpentinized oceanic peridotites: serpentinization processes and microbial sulfate reduction. J. Geophys. Res. 103, 9917–9929.

Andersen, T., Griffin, W.L., O'Reilly, S.Y., 1987. Primary sulfide melt inclusions in mantle-derived megacrysts and pyroxenites. Lithos 20, 279–295.

Büchl, A., Brugmann, G., Batanova, V.G., Munker, C., Hofmann, A.W., 2002. Melt percolation monitored by Os isotopes and HSE abundances: a case study from the mantle section of the Troodos Ophiolite. Earth Planet. Sci. Lett. 204, 385–402.

Bach, W., Garrido, C.J., Paulick, H., Harvey, J., Rosner, M., 2004. Seawater-peridotite interactions: first insights from ODP Leg 209, MAR 15° N. Geochem. Geophys. Geosyst. 5.

Ballhaus, C., Bockrath, C., Wohlgemuth-Ueberwasser, C., Laurenz, V., Berndt, J., 2006. Fractionation of the noble metals by physical processes. Contrib. Mineral. Petrol. 152, 667–684.

Becker, H., Horan, M.F., Walker, R.J., Gao, S., Lorand, J.P., Rudnick, R.L., 2006. Highly siderophile element composition of the Earth's primitive upper mantle: constraints from new data on peridotite massifs and xenoliths. Geochim. Cosmochim. Acta 70, 4528–4550.

Birck, J.-L., Roy-Barman, M., Capmas, F., 1997. Re–Os isotopic measurements at the femtomole level in natural samples. Geostand. Newsl. 21, 19–27.

Bockrath, C., Ballhaus, C., Holzheid, A., 2004. Fractionation of the platinum-group elements during mantle melting. Science 305, 1951–1953.

Brügmann, G.E., Yang, J.-H., Snow, J.E., Rehkämper, M., Mezger, K., 1999. Gemeinsame Bestimmung der Os-Isotopie und der Edelmetall-konzentrationen in Peridotiten, Basalten, Sulfiden und Eisenmeteoriten. Kolloquium des DFG Schwerpunktprogramms 'Ocean drilling Programm and Deep Sea Drilling Project', Tagungsprogramm und Abstracts, pp. 21–22.

Chou, C.-L., 1978. Fractionation of siderophile elements in the Earth's upper mantle. Proc. Lunar Planet. Sci. 9, 219–230.

Cottrell, E., Walker, D., 2006. Constraints on core formation from Pt partitioning in mafic silicate liquids at high temperatures. Geochim. Cosmochim. Acta 70, 1565–1580.

Dick, H.J.B., Bullen, T., 1984. Chromian spinel as a petrogenetic indicator in abyssal and alpine-type peridotites and spatially associated lavas. Contrib. Mineral. Petrol. 86, 54–76.

Dromgoole, E.L., Pasteris, J.D., 1987. Interpretation of the sulfide assemblages in a suite of xenoliths from Kilbourne Hole, New Mexico. Geological Society of American, Special Paper.

Elthon, D., 1992. Chemical trends in abyssal peridotite: refertilization of depleted suboceanic mantle. J. Geophys. Res. 97, 9015–9025.

Ertel, W., Walter, M.J., Drake, M.J., Sylvester, P.J., 2006. Experimental study of platinum solubility in silicate melt to 14 GPa and 2273 K: implications for accretion and core formation in Earth. Geochim. Cosmochim. Acta 70, 2591–2602.

Fleet, M.E., Stone, W.E., Crocket, J.H., 1991. Partitioning of palladium, iridium, and platinum between sulfide liquid and basalt melt — effects of melt composition, concentration, and oxygen fugacity. Geochim. Cosmochim. Acta 55, 2545–2554.

Fleet, M.E., Crocket, J.H., Liu, M.H., Stone, W.E., 1999. Laboratory partitioning of platinum-group elements (PGE) and gold with application to magmatic sulfide-PGE deposits. Lithos 47, 127–142.

Griffin, W.L., Graham, S., O'Reilly, S.Y., Pearson, N.J., 2004. Lithosphere evolution beneath the Kaapvaal Craton: Re–Os systematics of sulfides in mantle-derived peridotites. Chem. Geol. 208, 89–118.

Hellebrand, E., Snow, J.E., Dick, H.J.B., Hofmann, A.W., 2001. Coupled major and trace elements as indicators of the extent of melting in mid-ocean-ridge peridotites. Nature 410, 677–681.

Holzheid, A., Sylvester, P., O'Neill, H.S.C., Rubie, D.C., Palme, H., 2000. Evidence for a late chondritic veneer in the Earth's mantle from high-pressure partitioning of palladium and platinum. Nature 406, 396–399.

Horan, M.F., Walker, R.J., Morgan, J.W., Grossman, J.N., Rubin, A.E., 2003. Highly siderophile elements in chondrites. Chem. Geol. 196, 5–20.

Ionov, D.A., Hoefs, J., Wedepohl, K.H., Wiechert, U., 1992. Contents and isotopic composition of sulfur in ultramafic xenoliths from central Asia. Earth Planet. Sci. Lett. 111, 269–286.

Ionov, D.A., Shirey, S.B., Weis, D., Brugmann, G., 2006. Os–Hf–Sr–Nd isotope and PGE systematics of spinel peridotite xenoliths from Tok, SE Siberian craton: effects of pervasive metasomatism in shallow refractory mantle. Earth Planet. Sci. Lett. 241, 47–64.

Jagoutz, E., Palme, H., Baddenhausen, H., Blum, K., Cendales, M., Dreibus, G., Spettel, B., Waenke, H., Lorenz, V., 1979. The abundances of major, minor and trace elements in the earth's mantle as derived from primitive ultramafic nodules. Lunar Planet. Sci. Conf. 10, 2031–2050.

Jochum, K.P., 1996. Rhodium and other platinum-group elements in carbonaceous chondrites. Geochim. Cosmochim. Acta 60, 3353–3357.

Jokat, W., Ritzmann, O., Schmidt-Aursch, M.C., Drachev, S., Gauger, S., Snow, J., 2003. Geophysical evidence for reduced melt production on the Arctic ultraslow Gakkel mid-ocean ridge. Nature 423, 962–965.

Jones, J.H., Drake, M.J., 1986. Geochemical constraints on core formation in the Earth. Nature 322, 221–228.

Kelemen, P.B., Dick, H.J.B., Quick, J.E., 1992. Formation of harzburgite by pervasive melt rock reaction in the upper mantle. Nature 358, 635–641.

Le Roux, V., Bodinier, J.L., Tommasi, A., Alard, O., Dautria, J.M., Vauchez, A., Riches, A.J.V., 2007. The Lherz spinel lherzolite: refertilized rather than pristine mantle. Earth Planet. Sci. Lett. 259, 599–612.

Lee, C.T.A., 2002. Platinum-group element geochemistry of peridotite xenoliths from the Sierra Nevada and the Basin and Range, California. Geochim. Cosmochim. Acta 66, 3987–4005.

Liu, C.Z., Snow, J.E., Hellebrand, E., Brügmann, G.E., von der Handt, A., Büchl, A., Hofmann, A.W., 2008. Ancient, highly heterogeneous mantle beneath Gakkel Ridge, Arctic Ocean. Nature 452, 311–316.

Lorand, J.P., Alard, O., 2001. Platinum-group element abundances in the upper mantle: new constraints from in situ and whole-rock analyses of Massif Central xenoliths (France). Geochim. Cosmochim. Acta 65, 2789–2806.

Lorand, J.P., Gregoire, M., 2006. Petrogenesis of base metal sulphide assemblages of some peridotites from the Kaapvaal craton (South Africa). Contrib. Mineral. Petrol. 151, 521–538.

Lorand, J.P., Keays, R.R., Bodinier, J.L., 1993. Copper and noble-metal enrichments across the lithosphere asthenosphere boundary of mantle diapirs — evidence from the Lanzo Lherzolite Massif. J. Petrol. 34, 1111–1140.

Lorand, J.P., Pattou, L., Gros, M., 1999. Fractionation of platinum-group elements and gold in the upper mantle: a detailed study in Pyrenean orogenic lherzolites. J. Petrol. 40, 957–981.

Lorand, J.P., Schmidt, G., Palme, H., Kratz, K.L., 2000. Highly siderophile element geochemistry of the Earth's mantle: new data for the Lanzo (Italy) and Ronda (Spain) orogenic peridotite bodies. Lithos 53, 149–164.

Lorand, J.P., Reisberg, L., Bedini, R.M., 2003. Platinum-group elements and melt percolation processes in Sidamo spinel peridotite xenoliths, Ethiopia, East African Rift. Chem. Geol. 196, 57–75.

Lorand, J.P., Delpech, G., Gregoire, M., Moine, B., O'Reilly, S.Y., Cottin, J.Y., 2004. Platinum-group elements and the multistage metasomatic history of Kerguelen lithospheric mantle (South Indian Ocean). Chem. Geol. 208, 195–215.

Lorand, J.P., Luguet, A., Alard, O., 2008. Platinum-group elements: a new set of key tracers for the Earth's interior. Elements 4, 247–252.

Luguet, A., Alard, O., Lorand, J.P., Pearson, N.J., Ryan, C., O'Reilly, S.Y., 2001. Laser-ablation microprobe (LAM)-ICPMS unravels the highly siderophile element geochemistry of the oceanic mantle. Earth Planet. Sci. Lett. 189, 285–294.

Luguet, A., Lorand, J.P., Seyler, M., 2003. Sulfide petrology and highly siderophile element geochemistry of abyssal peridotites: a coupled study of samples from the Kane Fracture Zone (45° W 23°20 N, MARK Area, Atlantic Ocean). Geochim. Cosmochim. Acta 67, 1553–1570.

Luguet, A., Lorand, J.P., Alard, O., Cottin, J.Y., 2004. A multi-technique study of platinum group element systematic in some Ligurian ophiolitic peridotites, Italy. Chem. Geol. 208, 175–194.

Luguet, A., Shirey, S.B., Lorand, J.-P., Horan, M.F., Carlson, R.W., 2007. Residual platinum-group minerals from highly depleted harzburgites of the Lherz massif (France) and their role in HSE fractionation of the mantle. Geochim. Cosmochim. Acta 71, 3082–3097.

McDonough, W.F., Sun, S.S., 1995. The composition of the Earth. Chem. Geol. 120, 223–253.

Meisel, T., Walker, R.J., Morgan, J.W., 1996. The osmium isotopic composition of the Earth's primitive upper mantle. Nature 383, 517–520.

Meisel, T., Walker, R.J., Irving, A.J., Lorand, J.P., 2001. Osmium isotopic compositions of mantle xenoliths: a global perspective. Geochim. Cosmochim. Acta 65, 1311–1323.

Michael, P.J., Langmuir, C.H., Dick, H.J.B., Snow, J.E., Goldstein, S.L., Graham, D.W., Lehnert, K., Kurras, G., Jokat, W., Muhe, R., Edmonds, H.N., 2003. Magmatic and

amagmatic seafloor generation at the ultraslow-spreading Gakkel ridge, Arctic Ocean. Nature 423, 956–961.
Morgan, J.W., 1986. Ultramafic xenoliths — clues to Earth's late accretionary history. J. Geophys. Res. 91, 2375–2387.
Morgan, J.W., Walker, R.J., Brandon, A.D., Horan, M.F., 2001. Siderophile elements in Earth's upper mantle and lunar breccias: data synthesis suggests manifestations of the same late influx. Meteoritics. Planet. Sci. 36, 1257–1275.
Murthy, V.R., 1991. Early differentiation of the earth and the problem of mantle siderophile elements — a new approach. Science 253, 303–306.
O'Neill, H.S., 1991. The origin of the Moon and the early history of the Earth — a chemical model 2: the Earth. Geochim. Cosmochim. Acta 55, 1159–1172.
Palme, H., O'Neill, H.S.C., 2004. Cosmochemical estimate of mantle composition. In: Carlson, R.W. (Ed.), The Mantle 2. Elsevier, Oxford, pp. 1–38.
Pattou, L., Lorand, J.P., Gros, M., 1996. Non-chondritic platinum-group element ratios in the Earth's mantle. Nature 379, 712–715.
Pearson, D.G., Irvine, G.J., Ionov, D.A., Boyd, F.R., Dreibus, G.E., 2004. Re–Os isotope systematics and platinum group element fractionation during mantle melt extraction: a study of massif and xenolith peridotite suites. Chem. Geol. 208, 29–59.
Peregoedova, A., Barnes, S.-J., Baker, D.R., 2004. The formation of Pt–Ir alloys and Cu–Pd-rich sulfide melts by partial desulfurization of Fe–Ni–Cu sulfides: results of experiments and implications for natural systems. Chem. Geol. 208, 247–264.
Rehkämper, M., Halliday, A.N., 1997. Development and application of new ion-exchange techniques for the separation of the platinum group and other siderophile elements from geological samples. Talanta 44, 663–672.
Rehkämper, M., Halliday, A.N., Barfod, D., Fitton, J.G., 1997. Platinum-group element abundance patterns in different mantle environments. Science 278, 1595–1598.
Rehkämper, M., Halliday, A.N., Alt, J., Fitton, J.G., Zipfel, J., Takazawa, E., 1999. Non-chondritic platinum-group element ratios in oceanic mantle lithosphere; petrogenetic signature of melt percolation? Earth Planet. Sci. Lett. 172, 65–81.
Reisberg, L., Lorand, J.P., 1995. Longevity of subcontinental mantle lithosphere from osmium isotope systematics in orogenic peridotite massifs. Nature 376, 159–162.
Righter, K., Drake, M.J., 1997. Metal-silicate equilibrium in a homogeneously accreting earth: New results for Re. Earth Planet. Sci. Lett. 146, 541–553.
Saal, A.E., Takazawa, E., Frey, F.A., Shimizu, N., Hart, S.R., 2001. Re–Os isotopes in the Horoman peridotite: evidence for refertilization? J. Petrol. 42, 25–37.
Schmidt, G., Palme, H., Kratz, K.L., Kurat, G., 2000. Are highly siderophile elements (PGE, Re and Au) fractionated in the upper mantle of the earth? New results on peridotites from Zabargad. Chem. Geol. 163, 167–188.
Seyler, M., Toplis, M.J., Lorand, J.P., Luguet, A., Cannat, M., 2001. Clinopyroxene microtextures reveal incompletely extracted melts in abyssal peridotites. Geology 29, 155–158.
Shirey, S.B., Walker, R.J., 1998. The Re–Os isotope system in cosmochemistry and high-temperature geochemistry. Annu. Rev. Earth Planet. Sci. 26, 423–500.
Snow, J.E., Dick, H.J.B., 1995. Pervasive magnesium loss by marine weathering of peridotite. Geochim. Cosmochim. Acta 59, 4219–4235.
Snow, J.E., Schmidt, G., 1998. Constraints on Earth accretion deduced from noble metals in the oceanic mantle. Nature 391, 166–169.
Snow, J.E., Petrology-Group-ARK-XX-2, 2007. Petrology of Lena Trough and Gakkel Ridge. Reports on Polar and Marine Research, vol. 544, pp. 153–208.
Stone, W.E., Crockett, J.H., Fleet, M.E., 1990. Partitioning of palladium, iridium, platinum and gold between sulfide liquid and basalt melts at 1200 °C. Geochim. Cosmochim. Acta 54, 2341–2344.
van Acken, D., Becker, H., Walker, R.J., 2008. Refertilization of Jurassic oceanic peridotites from the Tethys Ocean — implications for the Re–Os systematics of the upper mantle. Earth Planet. Sci. Lett. 268, 171–181.